

Article

SIW Leaky Wave Antenna for THz Applications

Vivek Arya ^{1,*}, Tanuj Garg ¹ and Hamza Mohammed Ridha Al-Khafaji ^{2,*}¹ Department of ECE, FET, Gurukula Kangri (Deemed to Be University), Haridwar 249404, Uttarakhand, India² Biomedical Engineering Department, Al-Mustaqbal University College, Hillah 51001, Babil, Iraq

* Correspondence: ichvivekmalik@gmail.com (V.A.); hamza.alkhafaji@uomus.edu.iq (H.M.R.A.-K.)

Abstract: This paper proposes a new design of leaky wave antenna (LWA) based on substrate integrated waveguide (SIW) technology for THz applications. The suggested LWA structure has a combination of longitudinal and transverse slots and makes a 10-element linear array of radiating elements. To address the problem of open-stop-band (OSB), four additional smaller slots were etched on the corners of longitudinal and transversal slots. At the broadside, this LWA provided a gain of 12.33 dBi, and a continuous wide beam scanning range from +78° to −6° via the broadside while exhibiting efficient radiation performance over the operating frequency bands of 105 GHz to 109 GHz with a peak gain of 16.02 dBi.

Keywords: leaky wave antenna (LWA); THz applications; SIW; CBS

1. Introduction

In 1940, a leaky wave antenna (LWA) was investigated as a rectangular type of closed waveguide structure [1]. The presence of slots at regular intervals on an electromagnetic wave-carrying waveguide results in the emission of a plane wave from these slots. Later, in 1956, N. Marcuvitz named this plane wave the leaky wave [2]. LWAs are waveguides with periodic slots that are responsible for the production of leaky waves [3]. In general, LWAs are made up of waveguides with a single/double radiator in a unit cell. Owing to its high gain, elementary structure, as well as its inherent beam scanning feature w.r.t. frequency, the type of traveling wave antenna is a planar LWA. LWA has a large range of applications in the fields of broadband free-space communications as well as collision-avoidance radars. LWAs are a sort of frequency beam scanning antenna that may be loosely categorized into three kinds, specifically uniform [4,5], periodic [6–8], and quasi-periodic [9,10], depending on the modulations applied to the waveguide. Although it emits from the main space harmonics ($n = 0$), uniform and quasi-periodic antenna structures radiate only in an advance forward direction. Composite left/right-handed LWAs, on the other hand, are quasi-periodic structures that radiate with fundamental harmonic both in the forward and backward directions.

In the past, different variants of LWAs have been proposed by various researchers for beam scanning. The periodic and uniform LWAs scan only in one direction, that is, only in the forward direction. The traditional LWAs suffered from broadside radiation problems. Traveling wave LWAs transform into standing wave antennas at broadside frequencies. Continuous beam scanning (CBS) [11] is now possible with the introduction of composite left/right transmission lines metamaterial [12], although at the cost of difficulties in production, as a unit cell period is shorter than $\lambda_g < 4$. Various experts have obtained CBS for periodic LWAs by different methods, such as matching stubs, taking a quarter distance between pairs of identical elements, and using substrate integrated waveguide (SIW) [13]. SIW is the most significant breakthrough of the previous decade, bridging the gap between metallic waveguides and planar circuits [14]. When compared to rectangular waveguides, SIW offers the capabilities of a low profile, lightweightedness, and the ability to be simply constructed using conventional PCB technology. As a result, SIW has sparked



Citation: Arya, V.; Garg, T.; Al-Khafaji, H.M.R. SIW Leaky Wave Antenna for THz Applications. *Electronics* **2023**, *12*, 1839. <https://doi.org/10.3390/electronics12081839>

Academic Editors: Syed Muzahir Abbas and Yang Yang

Received: 20 February 2023

Revised: 24 March 2023

Accepted: 10 April 2023

Published: 12 April 2023



Copyright: © 2023 by the authors. Licensee MDPI, Basel, Switzerland. This article is an open access article distributed under the terms and conditions of the Creative Commons Attribution (CC BY) license (<https://creativecommons.org/licenses/by/4.0/>).

a lot of interest, and a variety of components employing this technology have been created. Half and full-mode substrate integrated waveguides efficiently work for CBS. Due to the simplicity of the SIW structure, many researchers have developed SIW-based LWAs for CBS that provide good scanning capability [14]. Ultimately, the SIW platform will be essential for producing larger scanning range LWAs.

LWAs have been extensively researched in the microwave spectrum and have recently been developed at THz frequencies. The LWA, in its most basic form, is a metallic waveguide that leaks radiation via a slot formed beside its length, while more complicated designs exist that use metamaterials. The radiating beam arises from the hole or slot at a frequency-dependent angle to contest the phases of both the propagating and free-space modes. Several of the issues connected with THz transmission, such as frequency division multiplexing, beam steering, radar-object tracking, and connection discovery, have been addressed using this one-to-one correlation between emission angle and frequency.

Over the years, there has been considerable interest in terahertz (THz) technologies owing to their potential for access to wideband wireless links. To address numerous difficulties related to THz wireless communications, LWAs that scale at THz frequencies (over 100 GHz) have been considered suitable candidates due to their authentic qualities, such as narrow beam, high gain, high efficiency, and wider CBS capabilities [15,16]. The SIW-based LWAs that work in the THz range have many important growing applications, such as high transmission rate communications [17], voice-recognizing radar systems [18], terrestrial remote sensing [19], as well as molecular spectroscopy [20].

A frequency scanning radiating device, i.e., an LWA, is a viable and efficient choice in this respect because of its straightforward feeding structure, excellent gain, and wide band nature [21,22]. The terms uniform and periodic refer to two types of LWAs, depending on the geometrical construction. For the uniform LWA, the waveguide must experience periodic disturbance in order to acquire leakage by leaky wave radiation. While in the periodic LWA structure, there is a constant perturbation along the waveguide structure. The primary beams of traditional uniform LWAs cannot be scanned in the backward quadrant space; however, LWAs with periodic structures have backward and forward scanning capabilities.

Nevertheless, the scanning area of a uniform LWA is limited to the front quadrant. The literature has described a number of perturbed guiding structures to date [23–25] in order to produce periodic LWAs. For their use in microwave and millimeter wave (mm-wave) applications, transverse metallic slotted waveguides, such as rectangular [23], substrate integrated [25,26], microstrip line [27,28], or coplanar [29], have been explored and achieved. However, LWA based on metallic waveguide is not a common option since there is a huge conductor loss and the creation of surface waves at higher frequencies exceeding 100 GHz [30]. Furthermore, their manufacturing is difficult since their sectional measurements must be 1/10th of the wavelength for a single-mode operation [31]. The majority of past studies, which built on previous work at minimum frequencies, used typical leaky-wave waveguide structures that may not be optimal for usage at THz frequency ranges. In the microwave range, for example, the leaky structural measurements are invariably deeply sub-wavelength in the span. This keeps the guided wave consistent through the slot width. Additionally, the radiated field pattern may be estimated in this limit, utilizing a simple mathematical model based on leakage rate as well as a sinc function. In contrast, the majority of modern THz implementations employ a leaky structure with a size close to the wavelength. At the wavelength scale, the wave interaction with the leaky structure can no longer be ignored to generate an output beam that follows the frequency-angle relationship; one must employ very tiny rectangular slots. This reduces device capability since the slot length radiated energy is quite short. This is a severe disadvantage, as the power production at THz frequencies remains a considerable issue. To address this issue, an alternative slot geometry, whereby the slot width rises linearly with its length, has been provided by various experts and has demonstrated that the design allows for improved coupling efficiencies at the output while maintaining the phase-matching

connection. Furthermore, because the trapezoidal slots have the larger effective aperture, the emitted beam is limited in both angular directions, which is notably not the case with a traditional rectangular slot aperture [18].

LWAs have been successfully developed utilizing a dielectric waveguide with enhanced loss characteristics to address these shortcomings at THz frequencies [32–41]. Different types of transmission lines called “dielectric waveguides” use one or additional insulating dielectrics to direct an electromagnetic wave. For more significant size reduction, different layers of dielectric material are typically employed. The waveguides that are based on dielectric have an inherent lack of conductor loss since their transmission mechanisms rely only on the reflections at the air and dielectric interfaces [42–44]. For high degrees of integration, a metal ground plane is a must when the waveguides are made from dielectric. One such transmission line is the dielectric image line (DIL), which has been employed in mm-wave as well as sub-THz circuits. It is perfectly integrated with the planar circuit. By focusing the electromagnetic energy at the interface of the dielectric, it considerably decreases the electric current on the ground plane and enables transmission with a significantly lower conductor loss [45].

Power leakages will occur when the DIL is perturbed on a regular basis as a semi-open structure as well as radiation, and can be generated deliberately to fulfill the needs of particular services. Numerous LWAs have been considered in recent literature to date on the basics of periodic DIL disturbances caused by metallic loadings or dielectric gratings. Due to the internal resonance, known as the open-stop-band (OSB) phenomenon, dielectric grating-based LWAs typically do not provide radiation in the precise broadside. Due to the various forms of dielectric grating, these LWAs also have manufacturing difficulties [32–40]. To circumvent the OSB problem, A.O. Salman [36] investigated the connection of sinusoidal metallic gratings having a dielectric line concave face. A second technique for producing leaky waves in a DIL environment is metallic perturbation on the surface of a DIL. The intrinsic ease of production and the audible radiation make this technology appealing. In [39], a leaky wave antenna was created using a regularly loaded DIL with rectangular metal strips. Beam scanning merely occurs in a forward direction in these LWAs. Five metal strips in a rectangular shape were utilized in a single unit cell in [40] to reduce the OSB phenomenon. This displays primary beam scanning between 80 and 120. Beam-scanning techniques other than LWAs, such as SIW edge-radiation, near-field transformation, and end-fire antennas, may be employed [40–50].

The design and optimization of such SIW-based leaky wave structures at THz frequencies need high computer computations due to complex calculations. A new SIW LWA in the THz frequency region is suggested in this paper, which is the foundation for the wider angle of scanning at THz. An array of periodic nature composed of metallic circular discs that overlapped each other was used in the suggested antenna between different dielectric layers to create a radiator of high efficiency having broadside OSB mitigation properties. The open-stop-band is the biggest challenge for leaky wave antennas. Generally, open-stop-band indicates the range of frequencies in the EM spectrum where radiation is stopped in a particular direction. As we know that LWA is a kind of directional antenna that produces radiation in a specific direction by allowing the propagation of waves in the antenna structure. The open-stop-band in an LWA is created by adding a periodic perturbation in the antenna structure. This perturbation results in a periodic variation of the guided wave’s effective refractive index along the antenna. When the wavelength of the guided wave matches the antenna’s periodicity, a strong reflection takes place that creates a stop band. In this stop band, the radiation waves will experience strong reflection and will not be allowed to propagate. As a result, the antenna beam pattern will exhibit a null in this direction and enhance the antenna’s directional properties. Various techniques are available for removing OSB issue, such as impedance matching, and the asymmetry, ridged, reflection cancellation, RC, and composite right/left-handed (CRLH) techniques. Generally, researchers used all these techniques to remove the OSB problem completely for the leaky wave antennas. The ridged technique is highly complex, but the RC and CRLH

techniques are less complex compared to others. From the perspective of performance, all the OSB removal techniques work effectively, while the impedance matching and CRLH techniques are highly efficient and show excellent performance. The CRLH transmission line (TL) is normally used for realizing backfire to end-fire LWA [13]. A special feature of this type of LWA, which cannot be obtained in conventional LWA, is the backfire-to-end-fire ability of LWA (uniform or periodic), which was first signified experimentally in [13,14]. SIW is a planar platform that demonstrates itself as an excellent possibility for the realization of CRLH LWAs. In OSB, the CRHL technique is most effective and gives qualitative results in broadside and perfect impedance matching at the broadside to remove OSB. Most of the techniques can remove the problem of OSB but do not achieve the best impedance bandwidth in the broadside for a restricted beam scanning range. Again, in the impedance matching technique, a SIW-based unit cell accommodates a longitudinal slot and inductive post, whose positions are opposite from the center of the unit cell. To achieve perfect impedance matching, a combination of longitudinal slots and inductive posts gives inductive and capacitive effects. In the top metallic plate, the longitudinal slots are located away from the midline for surface current radiation. The main lobe direction changes with frequency at the broadside direction [13,14]. No such complex techniques are used in the proposed antenna for the removal of OSB, while inherited slots solve this issue efficiently and effectively. The suggested antenna does not need elaborate prototyping and is light weight. The suggested design preserves most of the benefits of the aforementioned SIW-based LWAs, which have been successfully used at low mm-wave frequencies (<100 GHz), incorporating continuous broad beam-scanning abilities with OSB suppression employing a low-profile construction and cheap cost.

2. Design Methodology and Antenna Array

The proposed SIW-based LWA configuration for THz applications is depicted in Figure 1. In this, the longitudinal and transverse slots are integrated with SIW along with a feed network. First, we designed the SIW platform for the design of a SIW leaky wave antenna for THz applications.

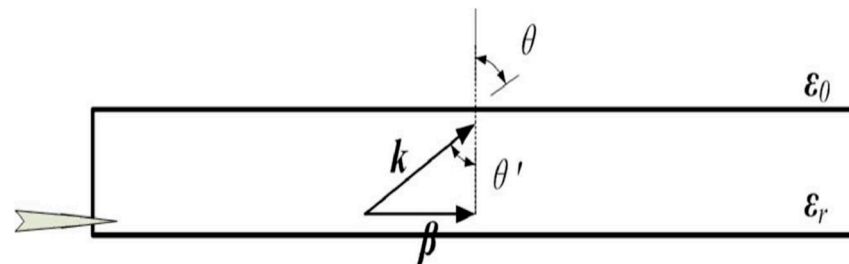


Figure 1. Side elevation of a leaky wave antenna.

2.1. Design of SIW

The side elevation for LWA along with its notations is shown in Figure 1, in which k denotes the propagation constant and β represents the phase constant for SIW, and they can be defined as [51–55]:

$$\sin \theta' = \frac{\beta}{k} \quad (1)$$

For simplifying the analysis, assume that when there is no leakage taking place, then β represents phase constant. The interface of dielectric and air medium refraction takes place following Snell's law as:

$$\frac{\sin \theta'}{\sin \theta} = \frac{1}{\sqrt{\epsilon_r}} \quad (2)$$

where ϵ_r represents the permittivity of the substrate material and with minimal attenuation, the pattern of the primary beam indicates an angle:

$$\theta = \arcsin \frac{\sqrt{\epsilon_r} \beta}{k} = \arcsin \frac{\beta}{k_0} = \arcsin \frac{\lambda_0}{\lambda_g} \quad (3)$$

In expression (3), k_0 represents the propagation constant, λ_0 represents the wavelength, and the guided wavelength of SIW is represented by λ_g . When leakage takes place, the value of β become less, hence β in SIW without any slot can be considered as the upper limiting case. Consider that the operating frequency is f and the required beam direction is θ , then:

$$\sin \theta = \sqrt{\epsilon_r - \left(\frac{c}{2wf} \right)^2} \quad (4)$$

where w means the width of SIW, and c represents light speed in free space. The dimension of SIW is the width (w) and it can be computed as [53]:

$$w = a - \frac{d^2}{0.95s} \quad (5)$$

where the diameter of via is (d) and the space between the two neighboring vias is called pitch and is denoted by (s). With the optimization procedure, the measured length is 6.25 mm and the width of the tapered line is 7.6 mm. In addition, Rogers substrate was utilized for the designing of the SIW-based LWA having 0.009 loss tangent, 0.787 mm thickness, and 2.2 dielectric permittivity.

2.2. Design Concept

Periodic LWAs for THz were created by adding periodic perturbations in the waveguide's top surface. Two slots were added for the perturbations, which was a combination of transverse and longitudinal slots. These transverse and longitudinal slots were used in our case for periodic modulation. Apart from these longitudinal and transverse slots, four additional smaller slots were also added, which removed the open-stop-band problem effectively without using any OSB removal techniques. These disturbances produced infinity of space harmonics. In periodic LWAs, just a single rapid harmonic should be emitted for only one beam creation. This rapid wave space harmonic (i.e., $n = -1$ and $n = 0$) generates a complicated leaky propagation constant that is steered down the line. There is an important relationship between the phase constant and period (P) of a unit cell [33]. Apart from these longitudinal and transverse slots, four additional smaller slots were also added, which removed the open-stop-band problem effectively without using any OSB removal techniques:

$$\beta_n = \beta_0 + \frac{2\pi n}{P} \quad (6)$$

where P denotes the period, and β_0 represents the fundamental phase constant.

The phase constant value varied from a -ve to +ve zero crossing. As a direct consequence of this backward or negative, side-to-forward or positive side scanning takes place. However, the radiation from such antenna designs at the broadside is constrained via an OSB, which results from the standing wave production at broadside frequency. This results in a poor radiation pattern as well as a significant return loss [34]. Again, the attenuation (α) and the phase constant (β) are the two key factors that are responsible for the design of the LWA. These factors may be utilized to determine the angle of the main beam from the broadside as:

$$\sin \theta = \frac{\beta}{k_0} \quad (7)$$

where θ denotes the main angle of the beam from the broadside, and k_0 represents the free space wave number. The length of the leaky wave antenna is thereby chosen ~90% of its energy and gets transmitted while reaching to load and is expressed by:

$$\frac{L}{\lambda_0} = \frac{0.18}{\alpha/k_0} \quad (8)$$

For the proposed design, $n = -1$ harmonic was produced by creating periodic modulations. For the broadside $\beta_{-1} = 0$, as per Equation (6) we then get:

$$\beta_0 = \frac{2\pi n}{P} = \frac{2\pi}{\lambda_g} \quad (9)$$

where λ_g denotes the guided wavelength. By Equation (9), we can say that to achieve the CBS unit cell period must be equivalent to the guided wavelength.

2.3. Geometry

The SIW LWA unit cell design and array design are illustrated in Figure 2a,b. The LWA was made up of 10 unit cells that resulted in 147 mm length. The unit cell of SIW design had dual artificial electric walls utilizing the vias. Also, the diameter 'd' as well as the spacing 's' (i.e., $\leq 2d$) between these vias was assumed to be 1 mm as well as 2 mm, correspondingly. Otherwise, the SIW width can be determined by Equation (5). The proposed LWA was ingested from the left side and a matched impedance via a 50 Ω termination was achieved. The unit cell dimensions are shown in Table 1. Furthermore, a unit cell dispersion diagram is represented by Figure 2c, which indicates that scanning took place from the back side to the forward side through the broadside.

Table 1. Parameters of a unit cell design.

Parameters	Values (mm)
P	14.7
W	16
A _L	5.5
A _T	3.6
D	1
B	0.8
C	1.5
S	2
W _{eff}	14

For the SIW design to work as an LWA, the rectangular slots were etched on the SIW's top surface. Four smaller additional slots were also made along with the longitudinal and transverse slots, which provide leaky wave radiation. The selected longitudinal and transverse slot was 90°, since the total power transmitted by these slots was equal to $\sin^2 \varphi$ where φ represents the angle of the intersection of the longitudinal and transverse slots.

To determine the angle between the longitudinal and transverse slots for the SIW LWA, a parametric analysis was carried out and the scattering parameter (S_{11}) is depicted in Figure 3. In the parametric analysis, to get the optimum scattering parameter, different angles between the longitudinal and transversal slots were applied, such as 70°, 80°, 90°, 100°, and 110°, as shown in Figure 3. As can be seen from Figure 3, the best scattering parameter plot was obtained when the angle between the longitudinal and transversal slots was 90°. For matching the antenna, the angle between the longitudinal and transverse slots was very important. The angle between the longitudinal and transverse slots must be 90 degrees to produce the optimum impedance matching and maximize the radiation from these slots. The nature of the electric field distribution for the proposed design

is represented by Figure 4, which shows the optimum distribution that is necessary for leaky waves.

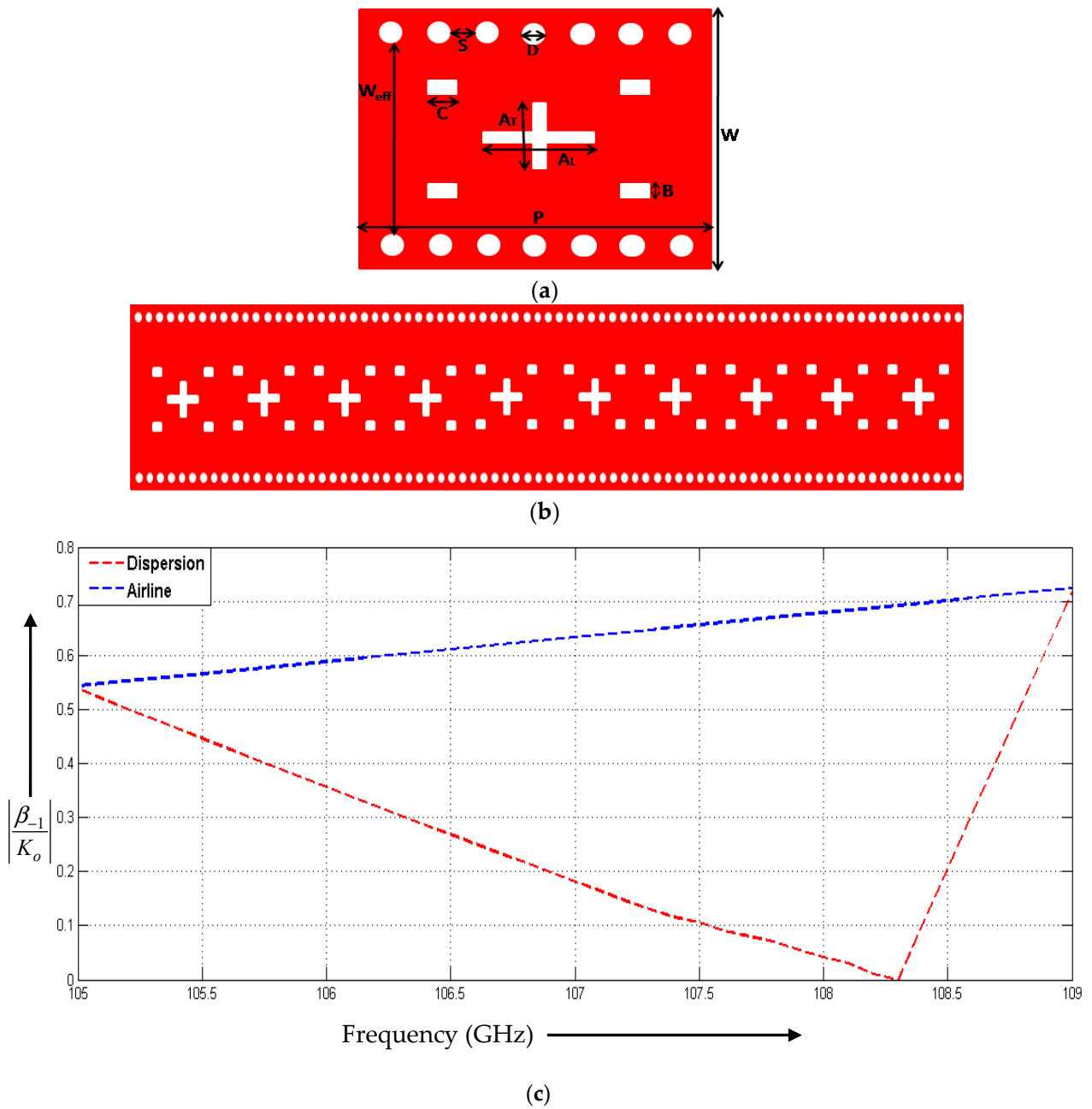


Figure 2. (a) SIW LWA unit cell, (b) SIW LWA structure, (c) Dispersion plot for a unit cell.

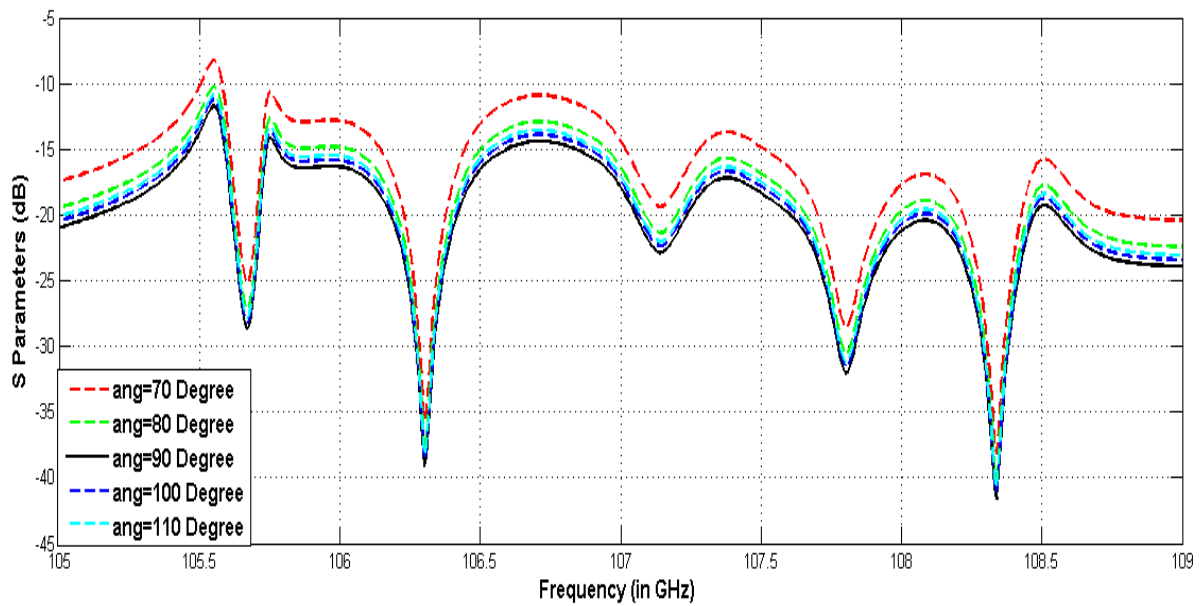


Figure 3. Parametric measurements for the angles between transversal and longitudinal slots at 70°, 80°, 90°, 100°, and 110°.

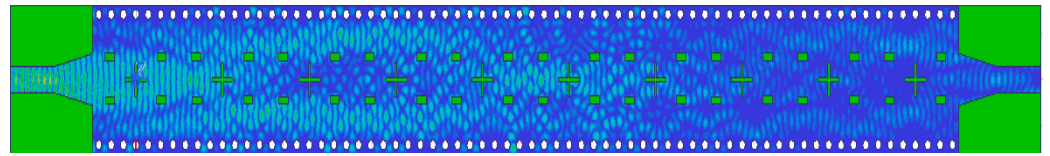


Figure 4. SIW electric field distribution.

3. Experiment Results

3.1. Geometry

An LWA for THz applications based on the SIW technology that gives CBS was designed. The SIW LWA structure for THz applications is depicted in Figure 2. The antenna was fed via a tapered microstrip line, which was terminated with a load matching the characteristic impedance. Using ANSYS HFSS software, the tapered part dimensions were optimized. The tapering line was 6.25 and 7.6 mm in length and breadth, respectively. The antenna's substrate had a tangent loss of 0.009, a height of 0.787 mm, and 2.2 dielectric permittivity.

3.2. S Parameters

Figure 5 depicts the reflection coefficient (S_{11}) for the designed SIWLWA. According to the simulated curve of the reflection coefficient (S_{11}) of the proposed antenna, the broadside (about 108.3 GHz) impedance matching was nearly perfect. As the open-stop-band issue is the biggest challenge for the researchers, the open-stop-band was removed perfectly during the simulation process without using any other components; as seen from Figure 5, there was no open-stop-band in the frequency range of 105 GHz to 109 GHz. The simulated results of the reflection coefficient (S_{11}) showed that this proposed leaky wave antenna worked well in the frequency band range of 105 GHz to 109 GHz.

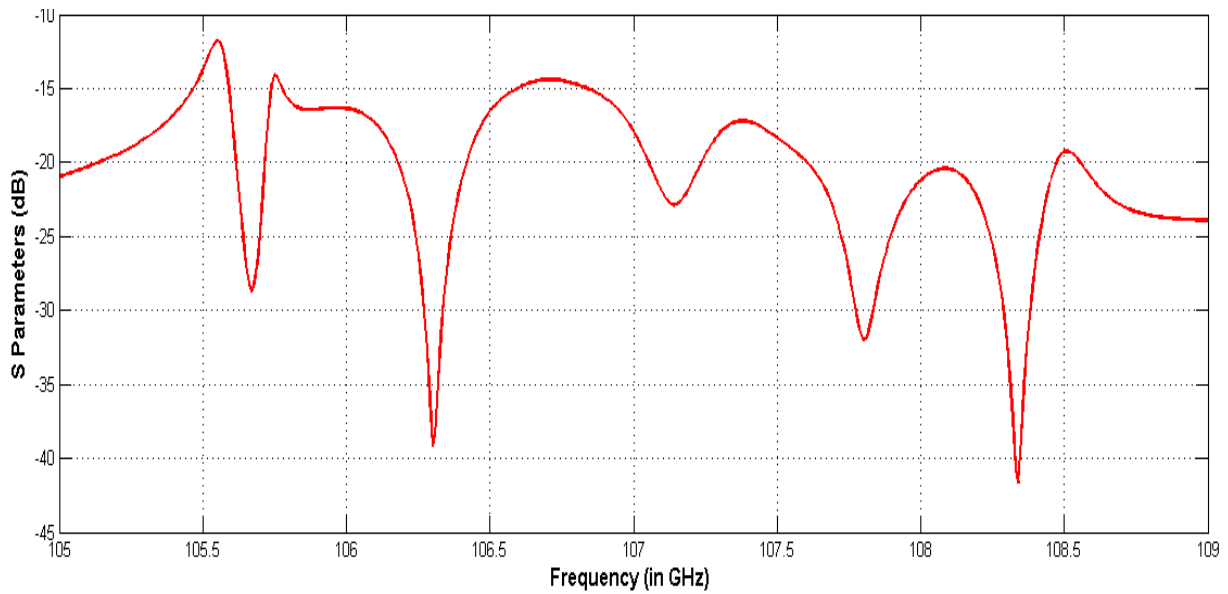


Figure 5. Simulated measured S_{11} parameter for SIW-LWA.

3.3. Radiation Features

For the simulation of the proposed antenna, the ANSYS HFSS software was utilized. First, the SIW and slots dimensions were optimized as per the frequency range, and after its simulation work was carried out. The simulated normalized radiation patterns of the suggested THz-based SIW LWA in y-z plane are depicted in Figure 6. The simulation for all the frequencies from 105 GHz to 109 GHz was performed by considering the difference of 0.5 GHz. When the frequency was swept in the 105~109 GHz range, the beam scanned from $+78^\circ$ to -6° for the SIW leaky wave antenna. The simulation yielded an entire beam scanning range of 84° . This beam went from $+78^\circ$ at 105 GHz via the broadside (108.3 GHz) to the rearward direction as well as pointed at -6° at 109 GHz with a rise in frequency. For the designed SIWLWA, this showed continuous beam scanning in the THz applications.

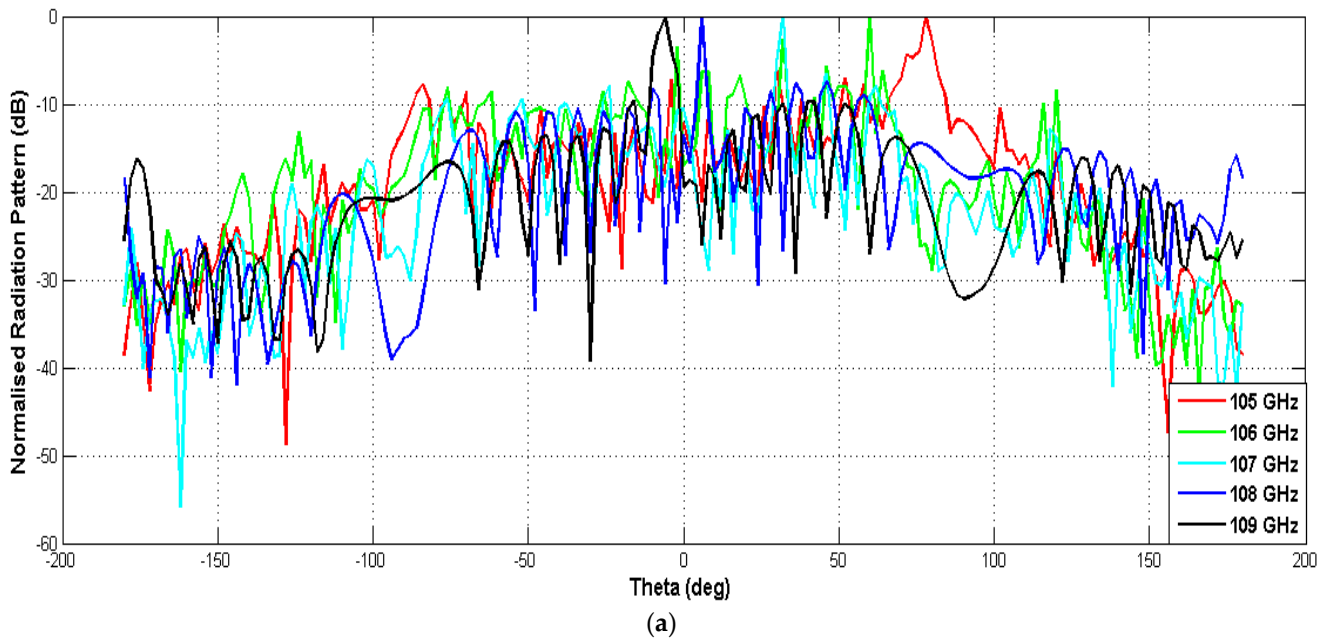


Figure 6. Cont.

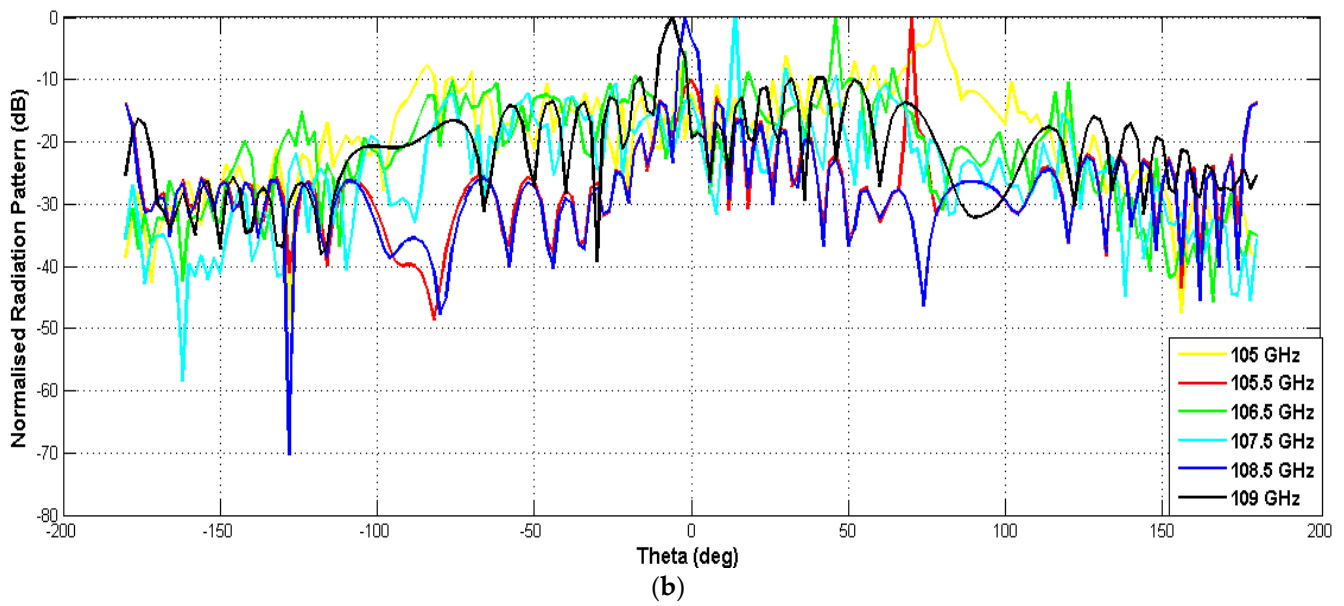


Figure 6. (a,b) Simulated 2D radiation patterns of SIW LWA in y-z plane.

The primary lobe directions for the proposed antenna are represented in Figure 7. The designed SIWLWA scanning range was higher than that of the current SIW-based THz leaky wave antennas, as the radiation from every longitudinal slot in the proposed SIW LWA disappeared at end-fire. As shown in Figure 7, at 108.3 GHz, scanning took place at 0 degrees (at broadside), after 108.3 GHz, scanning took place on the backward side, and before 108.3 GHz, scanning only occurred on the forward side. Figure 8 shows the simulated gain patterns for the SIWLWA and the maximum gain obtained was 16.02 dBi at 107 GHz; Table 2 shows that the recommended antenna was superior and more compact than other SIW-based leaky wave antennas for THz applications.

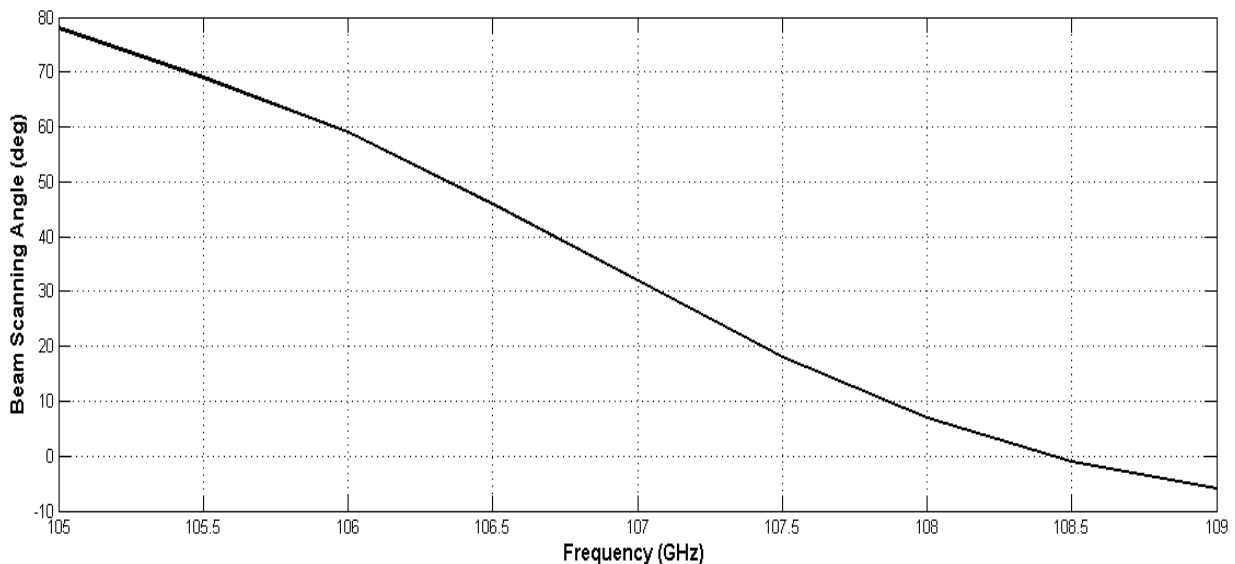


Figure 7. Various radiation angles for the proposed SIW LWA.

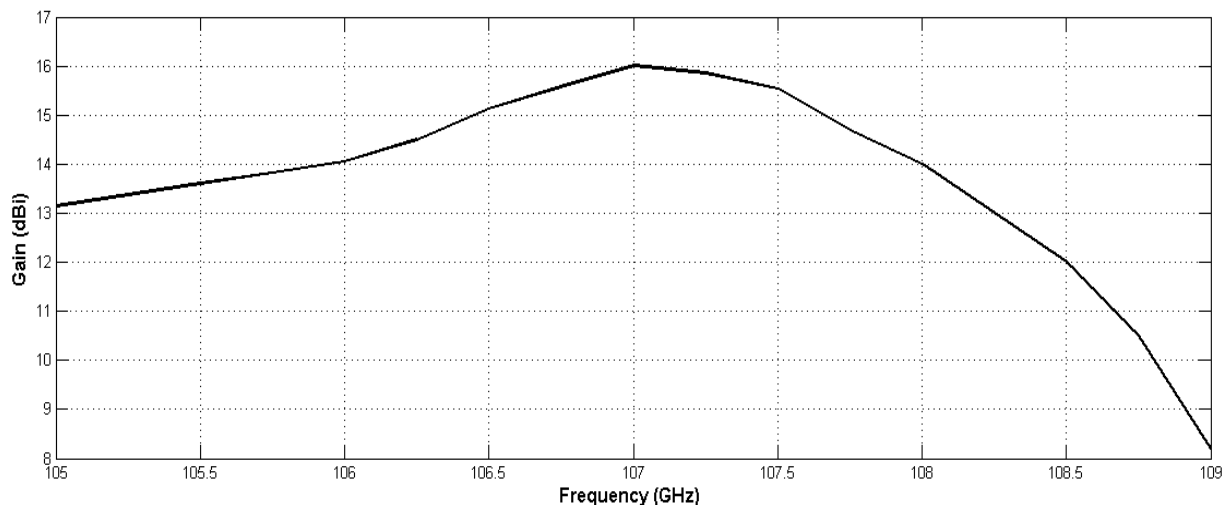


Figure 8. Simulated gain patterns for SIW LWA.

Table 2. Comparisons with other reported designs.

References	Broadside Radiation	Radiator Length	Range of Scanning Frequency (GHz)	Range of Beam Scanning (Degree)	Max. Gain
[15]	No	$\sim 10\lambda_0$	220 to 300	-75° to -30° (Backward Only)	~ 28.5 dBi
[38]	Yes	$\sim 11.1\lambda_0$	75 to 85	-10° to -8°	~ 12.7 dBi
[39]	No	$\sim 2.6\lambda_0$	58 to 67	$+7^\circ$ to $+38^\circ$ (Forward Only)	~ 11.7 dBi
[40]	Yes	$\sim 6\lambda_0$	86 to 106	-31° to $+10^\circ$	~ 11 dBi
[53]	No	$\sim 12\lambda_0$	55 to 67	4° to 18° (Forward Only)	~ 6 dBi
[54]	Yes	$\sim 8\lambda_0$	230 to 245	-25° to 25°	~ 29 dBi
[44]	Yes	$\sim 6.9\lambda_0$	157.5 to 206	-23° to $+38^\circ$	~ 15 dBi
This work	Yes	$\sim 6.84\lambda_0$	105 to 109	$+78^\circ$ to -6°	~ 16.02 dBi

3.4. Fabrication as Well as Measurement Issues

The recommended antenna design had a good structure operating as the LWA with outstanding characteristics in THz frequencies; nevertheless, its fabrication could be a little difficult. For instance, the expected air gap between the ground plane and the dielectric layer during manufacturing might result in minor differences between the simulation and measurement findings. Additionally, it might be difficult to achieve fewer reflection losses in THz frequencies since even a small variation in the feature sizes and the value of the dielectric constant can have a direct impact on antenna performance. Furthermore, because of technological restrictions, it could be difficult to measure the radiation patterns of the antenna throughout the whole 180° range. Indeed, the radiation pattern at such high frequencies can be altered at angles close to the backfire by a variety of sources of diffraction linked to antenna-feeding impacts (i.e., plastic screw, waveguide flange, etc.). Additionally, as most testing equipment is waveguide-based and operates at THz frequencies without connections, the transitions are crucial to the suggested design. A straightforward inline transition between the microstrip line and a rectangle waveguide may have been needed for the measurement in this study as the microstrip line was employed for feeding. The simulation did not include any representation of the transitions to rectangular waveguide.

4. Conclusions

In this work, a new LWA-based SIW technology was presented for CBS that provided a wider range of beam scanning with high gain. The proposed antenna system employed a SIW and a combination of longitudinal as well as transverse slots to address the OSB

issue supplied by this waveguide. A 10-element linear array of radiating elements was constructed. Specific features of the suggested design were reviewed, including its feeding network, radiation characteristics, and difficulties in its production and measurement. From the broadside direction, a gain of 12.33 dBi was attained. This antenna provided continuous beam scanning in the range of $+78^\circ$ to -6° via the broadside while exhibiting good radiation performance over the working frequency band of 105 GHz to 109 GHz, with a peak gain of 16.02 dBi. The THz leaky wave antenna put forth in this paper was easily adaptable for realization at higher frequencies.

Author Contributions: Conceptualization, V.A., T.G. and H.M.R.A.-K.; methodology, V.A. and H.M.R.A.-K.; software, V.A. and H.M.R.A.-K.; validation, V.A. and H.M.R.A.-K.; formal analysis, V.A. and T.G.; investigation, V.A. and T.G.; resources, V.A. and H.M.R.A.-K.; writing—original draft preparation, V.A., T.G. and H.M.R.A.-K.; writing—review and editing, V.A., T.G. and H.M.R.A.-K.; visualization, V.A. and T.G.; supervision, T.G.; project administration, T.G. All authors have read and agreed to the published version of the manuscript.

Funding: This research received no external funding.

Data Availability Statement: Not applicable.

Conflicts of Interest: The authors have no conflict of interest to declare.

References

1. Hansen, W.W. Radiating Electromagnetic Waveguide. U.S. Patent No. 2,402,622,1940, 26 November 1940.
2. Marcuvitz, N. On field representation in terms of leaky modes or eigenmodes. *IRE Trans.* **1956**, *4*, 192–194.
3. Nishida, S. Leaky wave antennas. *Electron. Commun. Jpn.* **1965**, *48*, 42–48.
4. Goldstone, L.O.; Oliner, A.A. Leaky-wave antennas—Part I: Rectangular waveguides. *IRE Trans. Antennas Propag.* **1959**, *7*, 307–319. [[CrossRef](#)]
5. Cheng, Y.J.; Hong, W.; Wu, K.; Fan, Y. Millimeter-wave substrate integrated waveguide long slot leaky-wave antennas and two-dimensional multibeam applications. *IEEE Trans. Antennas Propag.* **2011**, *59*, 40–47. [[CrossRef](#)]
6. Lyu, Y.; Member, S.; Liu, X. Leaky-wave antennas based on non-cutoff substrate integrated waveguide supporting beam scanning from backward to forward. *IEEE Trans. Antennas Propag.* **2016**, *64*, 2155–2164. [[CrossRef](#)]
7. Zhou, W.; Liu, J.; Long, Y. Investigation of shorting vias for suppressing the open stopband in an SIW periodic leaky-wave structure. *IEEE Trans. Microw. Theory Tech.* **2018**, *66*, 2936–2945.
8. Agrawal, R.; Belwal, P.; Gupta, S. Asymmetric substrate integrated waveguide leaky wave antenna with open stop band suppression and radiation efficiency equalization through broadside. *Radioengineering* **2018**, *27*, 409–416. [[CrossRef](#)]
9. Liu, J.; Jackson, D.R.; Long, Y. Substrate integrated waveguide (SIW) leaky-wave antenna with transverse slots. *IEEE Trans. Antennas Propag.* **2012**, *60*, 20–29. [[CrossRef](#)]
10. Liu, J.; Tang, X.; Li, Y.; Long, Y. Substrate integrated waveguide leaky-wave antenna with H-shaped slots. *IEEE Trans. Antennas Propag.* **2012**, *60*, 3962–3967. [[CrossRef](#)]
11. Liu, L.; Caloz, C.; Itoh, T. Dominant mode (DM) leaky wave antenna with backfire-to-endfire scanning capability. *Electronics Lett.* **2003**, *38*, 1414–1416. [[CrossRef](#)]
12. Caloz, C.; Itoh, T. *Electromagnetic Metamaterials: Transmission Line Theory and Microwave Applications: The Engineering Approach*; Wiley: Hoboken, NJ, USA, 2006.
13. Guglielmi, M.; Jackson, D. Broadside radiation from periodic leaky-wave antennas. *IEEE Trans. Antennas Propag.* **1993**, *41*, 31–37. [[CrossRef](#)]
14. Paulotto, S.; Baccarelli, P.; Frezza, F.; Jackson, D.R. A novel technique for open-stopband suppression in 1-D periodic printed leaky-wave antennas. *IEEE Trans. Antennas Propag.* **2009**, *57*, 1894–1906. [[CrossRef](#)]
15. Gomez-Torrent, A.; Garcia-Vigueras, M.; Le Coq, L.; Mahmoud, A.; Ettore, M.; Sauleau, R.; Oberhammer, J. A Low-Profile and High-Gain Frequency Beam Steering Subterahertz Antenna Enabled by Silicon Micromachining. *IEEE Trans. Antennas Propag.* **2020**, *68*, 672–682. [[CrossRef](#)]
16. Monnai, Y. Terahertz Radar Based on Leaky-Wave Coherence Tomography. In Proceedings of the 2020 Conference on Lasers and Electro-Optics Pacific Rim, CLEO-PR 2020—Proceedings, Sydney, Australia, 2–6 August 2020; pp. 1–2.
17. Rikkinen, K.; Kyosti, P.; Leinonen, M.E.; Berg, M.; Parssinen, A. THz Radio Communication: Link Budget Analysis toward 6G. *IEEE Commun. Mag.* **2020**, *58*, 22–27. [[CrossRef](#)]
18. Kwon, H.; Kim, Y.; Yoon, H.; Choi, D. Selective Audio Adversarial Example in Evasion Attack on Speech Recognition System. *IEEE Trans. Inf. Forensics Secur.* **2020**, *15*, 526–538. [[CrossRef](#)]
19. Brown, E.R. Fundamentals of Terrestrial Millimeter-Wave and THz Remote Sensing. *Int. J. High Speed Electron. Syst.* **2003**, *13*, 995–1097. [[CrossRef](#)]

20. Golubiatnikov, G.Y.; Koshelev, M.A.; Tsvetkov, A.I.; Fokin, A.P.; Glyavin, M.Y.; Tretyakov, M.Y. Sub-Terahertz High-Sensitivity High-Resolution Molecular Spectroscopy with a Gyrotron. *IEEE Trans. Terahertz Sci. Technol.* **2020**, *10*, 502–512. [[CrossRef](#)]
21. Guerboukha, H.; Shrestha, R.; Neronha, J.; Ryan, O.; Hornbuckle, M.; Fang, Z.; Mittleman, D.M. Efficient Leaky-Wave Antennas at Terahertz Frequencies Generating Highly Directional Beams. *Appl. Phys. Lett.* **2020**, *117*, 261103. [[CrossRef](#)]
22. Agarwal, R.; Agarwal, A.; Dwivedi, A.; Sharma, A. Leaky Wave Antenna for Millimeter Wave Utilization. *J. Phys. Conf. Ser.* **2021**, *1921*, 012026. [[CrossRef](#)]
23. Ghalibafan, J.; Hashemi, S.M. Leaky-Wave Centerline Longitudinal Slot Antenna Fed by Transversely Magnetized Ferrite. *IEEE Trans. Magn.* **2016**, *52*, 4000104. [[CrossRef](#)]
24. Zheng, D.; Lyu, Y.-L.; Wu, K. Transversely Slotted SIW Leaky-Wave Antenna Applications. *IEEE Trans. Antennas Propag.* **2020**, *68*, 4172–4185. [[CrossRef](#)]
25. Ranjan, R.; Ghosh, J. SIW-Based Leaky-Wave Antenna Supporting Wide Range of Beam Scanning Through Broadside. *IEEE Antennas Wirel. Propag. Lett.* **2019**, *18*, 606–610. [[CrossRef](#)]
26. Saghati, A.P.; Mirsalehi, M.M.; Neshati, M.H. A HMSIW Circularly Polarized Leaky-Wave Antenna With. *IEEE Trans. Antennas Propag.* **2014**, *13*, 451–454. [[CrossRef](#)]
27. Chen, Y.; Wang, K.; Li, Y.; Long, Y. Periodic Microstrip Leaky Wave Antenna with Double-Sided Shorting Pins and Pairs of Slots. *Int. J. Antennas Propag.* **2020**, *2020*, 7101752. [[CrossRef](#)]
28. Martinez-Ros, A.J.; Gómez-Tornero, J.L.; Goussetis, G. Planar Leaky-Wave Antenna with Flexible Control of the Complex Propagation Constant. *IEEE Trans. Antennas Propag.* **2012**, *60*, 1625–1630. [[CrossRef](#)]
29. Grbic, A.; Eleftheriades, G.V. Leaky CPW-Based Slot Antenna Arrays for Millimeter-Wave Applications. *IEEE Trans. Antennas Propag.* **2002**, *50*, 494–1504. [[CrossRef](#)]
30. Alibakhshikenari, M.; Virdee, B.S.; Khalily, M.; Shukla, P.; See, C.H.; Abd-Alhameed, R.; Falcone, F.; Limiti, E. Beam-Scanning Leaky-Wave Antenna Based on CRLH-Metamaterial for Millimetre-Wave Applications Mohammad. *IET Microw. Antennas Propag.* **1941**, *74*, 535–546.
31. Pozar, D.M. *Microwave Engineering*, 4th ed.; John Wiley & Sons: Hoboken, NJ, USA, 2012; ISBN 978-0-470-63155-3.
32. Xu, S.; Gao, H. Double Dielectric Grating Leaky-Wave Antenna-Improved Perturbation Analysis. *Int. J. Infrared Millim. Waves* **1989**, *10*, 1103–1119. [[CrossRef](#)]
33. Hammad, H.F.; Antar, Y.M.; Freundorfer, A.P.; Sayer, M. Frequency. *IEEE Trans. Antennas Propag.* **2004**, *52*, 36–44. [[CrossRef](#)]
34. Bai, Y.; Liu, S. A Novel Dual-Beam Terahertz Leaky-Wave Antenna Based On Spoof Surface Plasmon Waveguide. *Optoelectron. Lett.* **2022**, *18*, 404–407. [[CrossRef](#)]
35. Choi, J.H.; Itoh, T. Beam-Scanning Leaky-Wave Antennas. In *Handbook of Antenna Technologies*; Chen, Z., Ed.; Springer: Singapore, 2015. [[CrossRef](#)]
36. Salman, A.O. On the antenna efficiencies for the dielectric leaky-wave antennas with a sinusoidal metallic diffraction grating coupled from the broad and the narrow face of the dielectric. *Microw. Opt. Technol. Lett.* **2011**, *53*, 2030–2034.
37. Aysu, B.; Filiz, G.; Merih, P.; Ozlem, T.; Peyman, M. 3D EM Data Driven Surrogate Based Design Optimization of Traveling Wave Antennas for Beam Scanning In X-Band: An Application Example. *Wirel. Netw.* **2022**, *28*, 1827–1834. [[CrossRef](#)]
38. Zandamela, A.; Al-Bassam, A.; Heberling, D. Circularly Polarized Periodic Leaky-Wave Antenna Based on Dielectric Image Line for Millimeter-Wave Radar Applications. *IEEE Antennas Wirel. Propag. Lett.* **2021**, *20*, 938–942. [[CrossRef](#)]
39. Cheng, Y.J.; Guo, Y.X.; Bao, X.Y.; Ng, K.B. Millimeter-Wave Low Temperature Co-Fired Ceramic Leaky-Wave Antenna and Array Based on the Substrate Integrated Image Guide Technology. *IEEE Trans. Antennas Propag.* **2014**, *62*, 669–676. [[CrossRef](#)]
40. Patrovsky, A.; Wu, K. Substrate Integrated Image Guide Array Antenna for the Upper Millimeter-Wave Spectrum. *IEEE Trans. Antennas Propag.* **2007**, *55*, 2994–3001. [[CrossRef](#)]
41. Liu, L.; Wang, J.; Yin, X.; Chen, Z.N. Wide-Angle Beam Scanning Leaky-Wave Antenna Using Spoof Surface Plasmon Polaritons Structure. *Electronics* **2018**, *7*, 348. [[CrossRef](#)]
42. Fuscaldo, W.; Zografopoulos, D.C.; Imperato, F.; Burghignoli, P.; Beccherelli, R.; Galli, A. Analysis and Design of Tunable THz 1-D Leaky-Wave Antennas Based on Nematic Liquid Crystals. *Appl. Sci.* **2022**, *12*, 11770. [[CrossRef](#)]
43. Sharma, J.; De, A. Full-Wave Analysis of Dielectric Rectangular Waveguides. *Prog. Electromagn. Res. M* **2010**, *13*, 121–131.
44. Torabi, Y.; Dadashzadeh, G.; Hadeie, M.; Oraizi, H.; Lalbakhsh, A. A Wide-Angle Scanning Sub-Terahertz Leaky-Wave Antenna Based on a Multilayer Dielectric Image Waveguide. *Electronics* **2021**, *10*, 2172.
45. Tesmer, H.; Razzouk, R.; Polat, E.; Wang, D.; Jakoby, R.; Maune, H. Temperature Characterization of Liquid Crystal Dielectric Image Line Phase Shifter for Millimeter-Wave Applications. *Crystals* **2021**, *11*, 63. [[CrossRef](#)]
46. Lalbakhsh, A.; Afzal, M.U.; Hayat, T.; Esselle, K.P.; Mandal, K. All-Metal Wideband Metasurface for near-Field Transformation of Medium-to-High Gain Electromagnetic Sources. *Sci. Rep.* **2021**, *11*, 9421. [[CrossRef](#)] [[PubMed](#)]
47. Mirmozafari, M.; Zhang, Z.; Gao, M.; Zhao, J.; Honari, M.M.; Booske, J.H.; Behdad, N. Mechanically Reconfigurable, Beam-Scanning Reflectarray and Transmitarray Antennas: A Review. *Appl. Sci.* **2021**, *11*, 6890, ISBN 0000000211512. [[CrossRef](#)]
48. Goudarzi, A.; Honari, M.M.; Gharaati; Mirzavand, R. A Cavity-Backed Antenna with a Tilted Directive Beam for 5G Applications. In Proceedings of the 2021 IEEE International Symposium on Antennas and Propagation and USNC-URSI Radio Science Meeting (APS/URSI), Singapore, 4–10 December 2021; pp. 1737–1738.
49. Afzal, M.U.; Matekovits, L.; Esselle, K.P.; Lalbakhsh, A. Beam-Scanning Antenna Based on near-Electric Field Phase Transformation and Refraction of Electromagnetic Wave through Dielectric Structures. *IEEE Access* **2020**, *8*, 199242–199253. [[CrossRef](#)]

50. Ibrahim, I.M.; Ahmed, M.I.; Abdelkader, H.M. A Novel Compact High Gain Wide-Band Log Periodic Dipole Array Antenna for Wireless Communication Systems. *J. Infrared Millim. Terahertz Waves* **2022**, *43*, 872–894. [[CrossRef](#)]
51. Kishihara, M.; Ohta, I.; Okubo, K.; Yamakita, J. Analysis of Post-Wall Waveguide Based on H-Plane Planar Circuit Approach. *IEICE Trans. Electron.* **2009**, *E92-C*, 63–71. [[CrossRef](#)]
52. Cassivi, Y.; Perregrini, L.; Arcioni, P.; Bressan, M.; Wu, K.; Conciauro, G. Dispersion Characteristics of Substrate Integrated Rectangular Waveguide. *IEEE Microw. Wirel. Compon. Lett.* **2002**, *12*, 333–335. [[CrossRef](#)]
53. Ghasemi, A.; Laurin, J.-J. A Continuous Beam Steering Slotted Waveguide Antenna Using Rotating Dielectric Slabs. *IEEE Trans. Antennas Propag.* **2021**, *67*, 6362–6370. [[CrossRef](#)]
54. Sarabandi, K.; Jam, A.; Vahidpour, M.; East, J. A Novel Frequency Beam-Steering Antenna Array for Submillimeter-Wave Applications. *IEEE Trans. Terahertz Sci. Technol.* **2018**, *8*, 654–665. [[CrossRef](#)]
55. Arya, V.; Garg, T.; Al-Khafaji, H.M.R. High Gain and Wide-Angle Continuous Beam Scanning SIW Leaky-Wave Antenna. *Electronics* **2023**, *12*, 370.

Disclaimer/Publisher’s Note: The statements, opinions and data contained in all publications are solely those of the individual author(s) and contributor(s) and not of MDPI and/or the editor(s). MDPI and/or the editor(s) disclaim responsibility for any injury to people or property resulting from any ideas, methods, instructions or products referred to in the content.